Adaptive holographic pumping of thin-film organic lasers

Citation for published version:
Wood, SM, Mavrogordatos, TK, Morris, SM, Hands, PJW, Castles, F, Atkinson, KL, Gardiner, DJ, Coles, HJ & Wilkinson, TD 2013, 'Adaptive holographic pumping of thin-film organic lasers', *Optics Letters*, vol. 38, no. 21, pp. 4483-4486. https://doi.org/10.1364/OL.38.004483

Digital Object Identifier (DOI):
10.1364/OL.38.004483

Published In:
Optics Letters

Adaptive holographic pumping of thin-film organic lasers

Simon M. Wood,[1] Themistoklis K. Mavrogordatos,[1] Stephen M. Morris,[1] Philip J. W. Hands,[2] Flynn Castles,[1] Damian J. Gardiner,[1] Katie L. Atkinson,[1] Harry J. Coles,[1] and Timothy D. Wilkinson[1,*]

[1]*Centre of Molecular Materials for Photonics and Electronics, Department of Engineering, University of Cambridge, 9 JJ Thomson Avenue, Cambridge CB3 0FA, UK*

[2]*School of Engineering, The University of Edinburgh, The King's Buildings, Mayfield Road, Edinburgh EH9 3JF, UK*

**Corresponding author: tdw13@cam.ac.uk*

Received August 7, 2013; revised September 25, 2013; accepted September 28, 2013; posted September 30, 2013 (Doc. ID 195325); published October 31, 2013

In this Letter, we use a reconfigurable hologram to dynamically control the position of incidence of the pump beam onto a liquid-crystal dye-based laser. The results show that there is an increase in the stability of the laser output with time and the average power when compared with the output of the same laser when it is optically excited using a static pump beam. This technique also provides additional functionality, such as wavelength tuning and spatial shaping of the pump beam, both of which are demonstrated here.

OCIS codes: (140.3490) Lasers, distributed-feedback; (140.2050) Dye lasers; (090.1970) Diffractive optics.
http://dx.doi.org/10.1364/OL.38.004483

Organic dye lasers are well established and are known to have a number of benefits, such as broadband wavelength tuning and high quantum efficiencies [1,2]. However, a significant disadvantage of using these lasers is that unwanted bleaching of the laser dye may occur, meaning it is generally necessary to reduce the interaction time between the dye molecules and the pump source to improve the output stability. One approach is to optically excite the dye using short timescale (e.g., nano- or picosecond) optical pulses with a low repetition rate (<1 kHz). However, to achieve higher repetition rates (>1 kHz) or continuous-wave operation, excited dye molecules must be removed from the pump volume. With liquid dye lasers, this may be performed with fluid flow [3], though generally at the cost of increased size and complexity. In thin-film and solid-state organic-dye lasers, a jet-stream approach is typically not viable, and, consequently, mechanical parts are required to physically translate the laser medium relative to the pump beam [4,5].

The purpose of this work is to demonstrate an alternative pumping technique for thin-film dye-based lasers in which a hologram is used to dynamically control the incident pump beam location. Such an approach negates the need for moving parts or dye circulation by moving the pump beam to ensure that the beam-dye interaction time remains short enough that unwanted bleaching effects can be avoided. These bleaching effects relate to any mechanism that removes excited dye molecules from the laser process and includes the buildup of triplet-triplet states and thermal degradation. For this demonstration, we used a chiral nematic liquid-crystal (LC) laser [6] that is doped with a fluorescent dye as a representative thin-film organic dye laser. The LC possesses a 1D photonic bandgap for visible light, which suppresses fluorescence in the bandgap [7] but enhances it at the band edges [8–11]. The dye acts as the gain medium; we have used a pyrromethene derivative since it is known to exhibit reduced triplet–triplet absorption, has a high quantum efficiency [12], and is soluble in LC media [13]. Previous work has shown that the illumination of a dye-doped chiral nematic LC with even relatively low-repetition-rate pump pulses can lead to a dramatic reduction in LC laser-output energies within a short timescale (~seconds) [14].

Figure 1(a) illustrates the principle of the adaptive pumping technique. The incident pump beam is produced by a Nd:YAG laser (CryLaS, FDSS 532-Q), which delivers 1 ns pulses at 532 nm and has a variable repetition rate up to 3000 Hz. The beam is reflected from a spatial light modulator (SLM) (SDE1280 LCOS) displaying a computer-generated hologram (CGH). From the SLM, the light is diffracted into a pattern defined by the hologram and then converted to the appropriate circular polarization in order to avoid reflection from the bandgap. It is then focused to form the replay field that will trigger lasing from the dye-doped chiral nematic LC cell. By changing the hologram displayed, different spot positions or patterns may be formed. This enables static pumping, in which the pump beam position remains

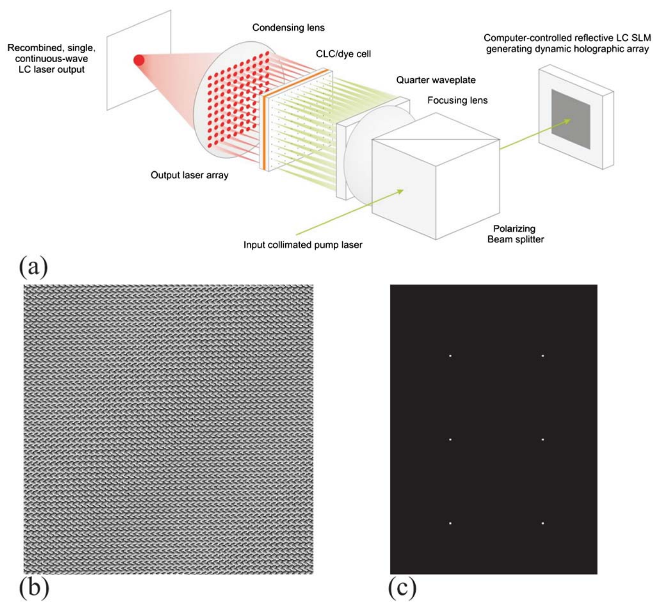

Fig. 1. Experimental setup and example hologram. (a) Illustration of the principle of dynamic optical pumping using computer-generated holograms. (b) Phase CGH (gray scale) used for the generation of six first-order spots in the replay field (768×768 pixels). (c) The ideal replay field.

fixed, and dynamic pumping, in which the pump beam position changes and fresh active gain regions are illuminated. The holograms displayed on the SLM were generated using the Gerchberg–Saxton phase-retrieval algorithm [15,16], which is frequently used in holographic applications. A CGH for a 2D array of six pump spots and its corresponding ideal replay field are shown as an example in Figs. 1(b) and 1(c).

In order to prove the principle of hologram-steered optical pumping, we created a hologram that would generate a single spot in the replay field. However, our SLM was not capable of true 2π modulation, meaning that a fraction of a conjugate image is formed in the replay field. This is because the Fourier transform of a real function is always 180° symmetric about the origin, as $|\psi(u,v)|^2 = |\psi(-u,-v)|^2$, where $\psi(u,v)$ is the complex amplitude of light in the diffraction plane. This reduces the efficiency of the hologram by 50%. Hence, if a hologram displayed on the SLM is used to generate a single first-order spot, there will actually be two first-order spots in the replay field. Thus, due to conjugate-image formation, two spatially separate pump beams were incident on the LC, and therefore two LC laser beams—corresponding to two spatially separated active regions—were generated. The emission spectrum [Fig. 2(a)] showed that the two separate LC laser beams emitted at the same wavelength: $\lambda = 560.2$ nm. In this case, the laser cell consisted of the nematic mixture E49 (Merck KGaA) doped with the chiral dopant BDH1281 (Merck KGaA; 3.5 wt. %) and the laser dye Pyrromethene 580 (PM-580; Exciton; 1 wt. %) to form a dye-doped chiral nematic LC. The cell had a thickness of 13 μm, which has been shown to be suitable for low-threshold lasing [17], and the spectrum was obtained using a universal serial bus spectrometer with a resolution of 0.3 nm (HR2000, Ocean Optics).

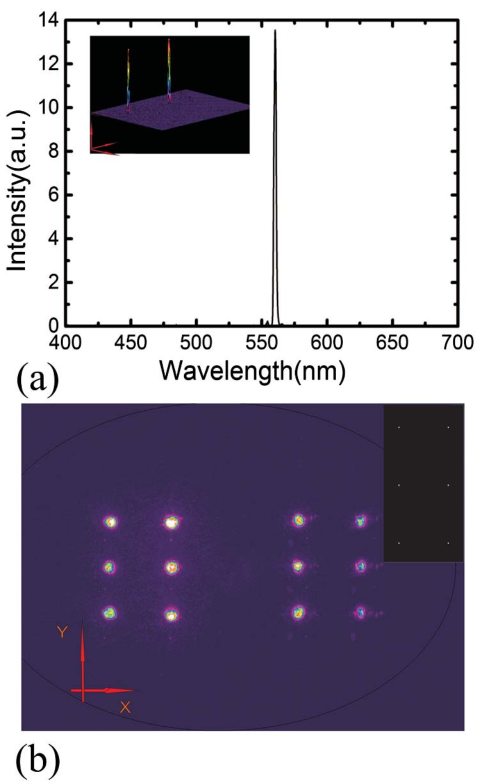

Fig. 2. Optically pumping a dye-doped LC laser using the replay field of a multilevel phase CGH. (a) Combined emission spectrum of a LC laser pumped by two spots in the replay field (inset: 3D intensity profile showing two spatially separated LC lasers). (b) 2D intensity profile for a LC laser array that is created using a CGH that generates 12 LC lasers (six spots plus the conjugate image).

The first-order pump spot in the replay field at the sample position was found to be approximately circular with an area of 0.003 mm^2. The excitation energy threshold was 130 nJ/pulse with a corresponding fluence of 4.3 $\mathrm{mJ/cm}^2$. Efficiencies for this system were found to be rather low ~2% due to the previously discussed limitations of the SLM. Since the hologram does not have a zero average, the constant term in the Fourier series is nonzero, and therefore a large amount of energy from the pump laser is redirected into a zero order, instead of the first orders that are used to create the LC laser. Previous reports for a similar LC laser have measured slope efficiencies of the order of 30% [13]. The spatial profile of the LC laser-beam intensity (captured using a Spiricon beam profiler) was recorded at a distance of 7 cm from the cell and found to be near Gaussian [Fig. 2(a)]. From this, beam widths were calculated to be approximately 70 μm at this distance from the cell. In addition, CGHs to generate spots in different positions and patterns were then created. An example of a 2D array of LC lasers (12 spots due to the presence of the conjugate image) is shown in Fig. 2(b). It should be noted that increasing the number of pumping spots results in a decrease of the pump intensity. This is because the first-order intensity in the replay field is now spread over more spots, and the amplitude of which follows an overall sinc envelope due to the square-shaped pixels of the SLM.

Subsequently, we demonstrate the benefits of dynamic pumping compared with static pumping. A sequence of holograms changing spot position every 0.5 s was created and used to steer the beam (Media 1). By scanning the beam around the lasing medium rapidly, so that it was only incident on a given active region for a short period of time, we ensured that unwanted bleaching effects were minimized. For this experiment, the pump energy as well as the energies of the pulses emitted from the LC laser were recorded using a calibrated pyroelectric head (PD10-SH-V2) connected to an energy meter (USB-2, Ophir). A suitable frame rate was determined by comparing several frame rates at a fixed repetition frequency [Fig. 3(a)]. A rate of 1 frame per second (fps) resulted in significant degradation of the output energy, while 2 fps gave a relatively stable output over several minutes. Increasing the rate to 10 fps did not lead to a significant improvement in stability but did reduce the output power as the fixed response time (>10 ms) of the nematic LC in the SLM had a more noticeable effect at higher frame rates.

When the LC laser was statically pumped with a single spot in a fixed location at different repetition rates [Fig. 3(b)], the normalized output energy decreased with the number of pulses, and the effect was more pronounced at higher repetition rates. At 600 Hz, the output dropped to 60% of its value in roughly 2000 pulses (4 s). It should be noted that increasing the repetition rate did

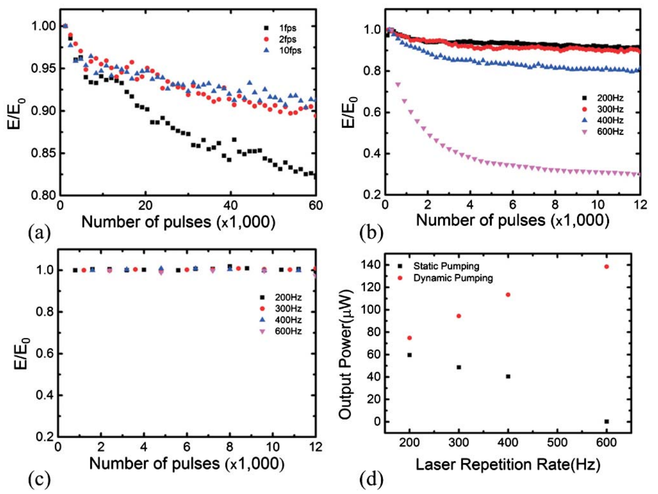

Fig. 3. Accessing higher repetition rates using dynamic pumping. The energy was recorded for each pulse, but in (a)–(c), the results are averaged over 2 s. The output energies are normalized to that recorded for the first pulse. (a) Dynamic pumping at 600 Hz with different SLM frame rates: 1 fps (■), 2 fps (•), and 10 fps (blue ▲). (b) Static pumping of a LC laser at different repetition rates. (c) Dynamic pumping with 2 fps at different repetition rates. In (b) and (c): 200 Hz (■), 300 Hz (•), 400 Hz (blue ▲), 600 Hz (pink ▼). (d) Total average output power over 1 min for different repetition rates for both the static (■) and dynamic (•) case.

not significantly alter the pump pulse energy. In contrast, when dynamic pumping is employed, the LC laser output is almost independent of pulse number, even at the highest repetition rate that we used; the output is significantly more stable [Fig. 3(c)]. For example, in the case of a 400 Hz repetition rate, it took 29 min to decay by 10%, compared with 5 s using static pumping.

The measured normalized photostabilities for the different repetition rates, corresponding to a 10% decrease in the output pulse energy and for the pumping volume in the LC cell based upon the cell thickness and pump spot area, are calculated to be 0.028 GJ/mol (200 Hz), 0.182 GJ/mol (300 Hz), 1.19 GJ/mol (400 Hz), and 1.41 GJ/mol (600 Hz). We also compared mean output powers over a given length of time [Fig. 3(d)], and this was greater at all repetition rates when dynamic pumping was employed. The mean output power for the first minute of emission increased with repetition rate when dynamically pumped, but decreased (due to bleaching) when statically pumped.

By combining the ability to steer the beam to different cell regions with a pitch-gradient LC cell—one that consists of a step-like continuum of wavelength-emitting regions—it was possible to tune the laser-emission wavelength [Fig. 4(a)] by accessing different gain regions and to create multicolor arrays [Fig. 4(b)]. The pitch-gradient cell, of 10 μm thickness, consisted of two different dye-doped LC mixtures, which are drawn into the cell by capillary action to form two regions gradually diffusing together and creating a continuous pitch gradient. Both of these mixtures comprised of the nematic LC, E49 (Merck), and the chiral dopant BDH1281 (Merck; 3.9 wt. % for red and 4.3 wt. % for green). DCM (Exciton; 1.5 wt. %) was added to make the red mixture, and PM580

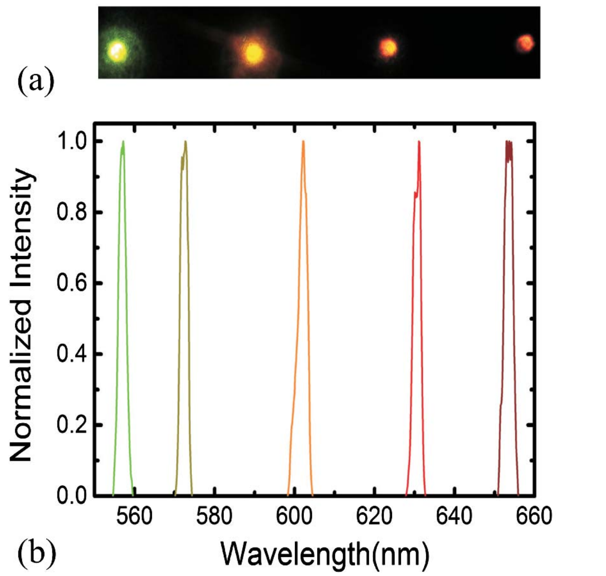

Fig. 4. Multicolor laser arrays and dynamic wavelength tuning. (a) Four spots (one zero order, two first order, and one second order) corresponding to different colors from red to green. (b) Emission spectra from different regions of the cell, obtained by static addressing of different spatial regions.

(Exciton; 0.5 wt. %) was added to make the green mixture. The method presented here can be directly applied to configurations relying on the energy-transfer between two dyes, allowing tunable output across the entire visible spectrum. Unlike previous approaches [18], this technique allows dynamically changing multicolor arrays to be created and, in contrast to previous work on lenslet arrays [19], the intensity of the spots in the array is independent of the spatial profile of the beam.

In conclusion, this Letter describes a system for pumping a dye-doped LC laser using computer-generated holography. The technique provides a means with which to vary the location of the pump beam on the active medium in real time, enabling fresh active gain regions to be addressed in rapid succession, thus reducing bleaching effects and improving thermal management. Dynamic pumping leads to improved stability, larger average output powers, and access to higher repetition rates when compared with static pumping. Using a simple algorithm to generate the holograms, the laser could be operated for hours at a repetition rate that would usually shut down laser operation within seconds due to photo bleaching. Furthermore, with this technique it is possible to precisely control the spatial wavefront, and configuration of the pumping wave and allows greater versatility and functionality to be realized. We have also demonstrated a simple approach to wavelength tuning and created simultaneous multichromatic outputs, but it is equally possible to envisage the creation of novel pump-beam profiles created to optimize propagation through the medium. Though we used a LC laser as a representative system, the work is equally applicable to other types of dye lasers, and the same approach could be used in the field of optically pumped organic semiconductor lasers.

The authors gratefully acknowledge the Engineering and Physical Sciences Research Council (UK) for financial support through the COSMOS research project (EP/H046658/1) and the Photonic Systems Development Centre for Doctoral Training. One of the authors (S. M. M.) gratefully acknowledges The Royal Society for financial support, and T. K. M. gratefully acknowledges the Foundation for Education and European Culture for financial support.

References

1. E. P. Schafer, ed., *Dye Lasers*, 3rd ed. (Springer-Verlag, 1990).
2. F. J. Duarte and L. W. Hillman, eds., *Dye Laser Principles* (Academic, 1990).
3. O. G. Peterson, S. A. Tuccio, and B. B. Snavely, Appl. Phys. Lett. **17**, 245 (1970).
4. R. Bornemann, U. Lemmer, and E. Thiel, Opt. Lett. **31**, 1669 (2006).
5. A. Costela, I. Garc-Moreno, R. Sastre, D. W. Coutts, and C. E. Webb, Appl. Phys. Lett. **79**, 452 (2001).
6. For a recent review, see H. J. Coles and S. M. Morris, Nat. Photonics **4**, 676 (2010).
7. E. Yablonovitch, Phys. Rev. Lett. **58**, 2059 (1987).
8. S. John, Phys. Rev. Lett. **58**, 2486 (1987).
9. J. P. Dowling, M. Scalora, M. J. Bloemer, and C. M. Bowden, J. Appl. Phys. **75**, 1896 (1994).
10. J. Schmidtke and W. Stille, Eur. Phys. J. B **31**, 179 (2003).
11. J. M. Bendickson, J. P. Dowling, and M. Scalora, Phys. Rev. E **53**, 4107 (1996).
12. T. G. Pavlopoulos, M. Shah, and J. H. Boyer, Opt. Commun. **70**, 425 (1989).
13. C. Mowatt, S. M. Morris, H. M. Song, T. D. Wilkinson, R. H. Friend, and H. J. Coles, J. Appl. Phys. **107**, 043101 (2010).
14. S. M. Morris, A. D. Ford, M. N. Pivnenko, and H. J. Coles, J. Opt. A **7**, 215 (2005).
15. R. W. Gerchberg and W. O. Saxton, Optik **35**, 237 (1972).
16. J. R. Fienup, Appl. Opt. **52**, 45 (2013).
17. S. M. Morris, A. D. Ford, C. Gillespie, M. N. Pivnenko, O. Hadeler, and H. J. Coles, J. Soc. Inf. Disp. **14**, 565 (2006).
18. S. M. Morris, P. J. W. Hands, S. Findeisen-Tandel, R. H. Cole, T. D. Wilkinson, and H. J. Coles, Opt. Express **16**, 18828 (2008).
19. P. J. W. Hands, S. M. Morris, T. D. Wilkinson, and H. J. Coles, Opt. Lett. **33**, 515 (2008).